

**Received:** 20.01.2025

**Accepted:** 19.02.2025

**Area of Expertise:** Forensic Medicine

**Title:** Determination of sex with occipital condyle measurements on three-dimensional computed tomography images.

**Short title:** Occipital condyle analysis for sex determination: 3D modelling.

### **Abstract**

**Purpose:** Morphometric measurements of cranial bones in skeletal remains are important for sex determination. Nowadays, radiological imaging techniques such as computed tomography are very useful in obtaining population-specific data. The aim of this study was to evaluate the usefulness of morphometric measurements of the occipital condyles in 3D cranial CT modeling for sex estimation in a Turkish population.

**Methods:** In this study, three-dimensional images of the occipital condyles were obtained by retrospectively using the carotid CT angiography images from the radiology department between 2019 and 2021. In these images, the length, width and height of both occipital condyles, distances between the basion with and the anterior and posterior ends of the occipital condyles, distances between the opisthion the anterior and posterior ends of the occipital condyles, anterior, posterior, minimum and maximum intercondylar distances, maximum bicondylar distance, right and left sagittal condylar angles, sagittal intercondylar angle, were measured.

**Results:** A statistically significant sexual dimorphism was found for all parameters except the left condylar angle measured in the occipital condyles. According to multivariate discriminant analysis models, sex could be estimated with an accuracy of 81.2% to 84.6% for males and 52.9% to 68.8% for females.

**Conclusion:** It was determined that three-dimensional computed tomography images of the occipital condyles can be used in sex estimation.

**Keywords:** Sex estimation, forensic anthropology, identification, occipital condyle, 3D modelling.

**Makale başlığı:** Üç Boyutlu bilgisayarlı tomografi görüntülerinde oksipital kondil ölçümleri ile cinsiyetin değerlendirilmesi.

**Kısa başlık:** Cinsiyet tahmini için oksipital kondillerin analizi: 3B modelleme.

**Öz**

**Amaç:** İskelet kalıntılarındaki kranial kemiklerin morfometrik ölçümleri cinsiyetin belirlenmesinde önemlidir. Günümüzde, bilgisayarlı tomografi gibi radyolojik görüntüleme teknikleri popülasyona özgü veriler elde etmede oldukça faydalıdır. Bu çalışmanın amacı, Türk popülasyonunda cinsiyet tahmini için 3B kranial BT modellemesinde oksipital kondillerin morfometrik ölçümlerinin yararlılığını değerlendirmektir.

**Gereç ve yöntem:** Bu amaçla, radyoloji anabilim dalı tarafından 2019-2021 yılları arasında çekilmiş karotis anjio BT görüntüleri retrospektif olarak kullanılarak oksipital kondillerin üç boyutlu görüntüleri elde edilmiştir. Bu görüntülerde her iki oksipital kondilin uzunluğu, genişliği ve yüksekliği, bazion ile oksipital kondilin ön ve arka uçları arasındaki mesafeler, opistion ile oksipital kondilin ön ve arka uçları arasındaki mesafeler, ön, arka, minimum ve maksimum interkondiler mesafeler, maksimum bikondiler mesafe, sağ ve sol sagittal kondiler açıları, sagittal interkondiler açı ölçülmüştür.

**Bulgular:** Sol kondiler açı dışındaki tüm parametrelerde cinsiyete göre istatistiksel olarak anlamlı farklılık olduğu ve oksipital kondillerde cinsel dimorfizm bulunduğu saptanmıştır. Diskriminant analizi ile oluşturulan çok değişkenli modellere göre erkeklerde %81,2 ile %84,6, kadınlarda ise %52,9 ile %68,8 doğrulukta cinsiyet tahmini yapılabileceği gösterilmiştir.

**Sonuç:** Oksipital kondillerin üç boyutlu bilgisayarlı tomografi görüntülerinin cinsiyet tahmininde kullanılabileceği saptanmıştır.

**Anahtar kelimeler:** Cinsiyet tahmini, adli antropoloji, kimliklendirme, oksipital kondil, 3B modelleme.

## **Introduction**

Human skeletal remains identification is one of the fundamental issues that require technical and expert knowledge covering many disciplines such as anatomy, radiology, archaeology, dentistry and genetics, which are of interest to physical anthropology as well as forensic medicine [1, 2]. The determination of the sex is one of the most important steps in the process of identification. This is because the methods to be used to determine other characteristics such as age and height estimation depend on the correct estimation of sex. It also eliminates half of the options in determining to whom the remains belong to [3, 4]. In cases of mass deaths such as natural disasters, wars, and major accidents, sex estimation becomes difficult due to fragmented and incomplete skeletal remains [5]. In this case, the reliability and accuracy of sex determination from skeletal remains depends on the anatomical region available [6].

The skull is the second best region for predicting sex after the pelvis, according to morphometric and morphological studies of the skull [7]. It is important to examine the base of the skull for sex estimation because the base of the skull may remain intact compared to other parts of the skull in various violent events such as fire, natural disasters and terrorist incidents due to its thickness and protected anatomical position [8, 9].

Computed tomography (CT) is increasingly used in forensic medicine [10]. It is stated that the use of CT images in the analysis of skeletal remains allows for faster evaluation, reduces the risks of deterioration, loss and similar risks of existing skeletal remains during transport, and allows for an opinion to be obtained by transmitting them to an expert anywhere in the world using information Technologies [11].

This study aimed to establish a standard for the morphometry of the occipital condyles (OC) on three-dimensional computed tomography (3DCT) models of the skull for sex estimation. Furthermore, the aim was to develop discriminant functions to investigate the potential use of occipital condyles in sex estimation in the contemporary Turkish population and to contribute to the occipital condyle database.

## **Material and methods**

This study was initiated following the granting of approval by the Ethics Committee for Non-Interventional Clinical Research of Pamukkale University (2021-E-60116787-020-49028). All procedures performed in studies were in accordance

with the ethical standards of the institutional and/or national research committee and with the 1964 Helsinki declaration and its later amendments or comparable ethical standards.

Carotid CT angiography images taken by the Department of Radiology between April 2019 and March 2021 were used retrospectively. A total of 481 (292 males and 189 females) images of the carotid CT angiography of individuals 18 years of age and older were included in the study. Scans with motion artefacts and cases with head trauma or joint pathology, such as arthrosis, were excluded. The carotid CT angiography investigations were made with the Philips Ingenuity 128 CT device and scans were obtained in 1 mm slices. The archived images were reloaded onto a standard work station (IntelliSpace Portal; release 10.1; Philips Medical Systems), and skull base images including the occipital condyles were obtained after a three-dimensional (3D) reconstruction was performed through bone window adjustments.

#### **Landmarks used in present study**

The basion (B), which is the point where the anterior edge of the foramen magnum (FM) meets the mid-sagittal line, the opisthion (O), which is the point where the posterior edge of FM meets the mid-sagittal line, and the anterior and posterior ends of the right and left OC determined in the horizontal plane are the landmarks determined for the evaluation (Figure 1).

#### **Morphometric measurement points of the occipital condyle on CCT images**

- **Occipital condyle length (OCL):** Maximum length along the long axis of the joint surfaces of the OCL (right and left)
- **Occipital condyle width (OCW):** Maximum width along a line vertical to the longitudinal axis of the articular surface of the OC (right and left)
- **Condylar index (Baudoin condylar index, BCI):**  $OCW / OCL \times 100$  (right and left)
- **Occipital condyle height (OCH):** The thickness at the intersection of the lines used to measure OCL and OCW (right - left)
- **Anterior intercondylar distance (AID):** Distance between the anterior ends of the joint surfaces of the right and left OC
- **Posterior intercondylar distance (PID):** Distance between the posterior ends of the joint surfaces of the right and left OC
- **Minimum intercondylar distance (MinID):** Minimum distance between medial joint surface edges of both OCs
- **Maximum intercondylar distance (MaxID):** Maximum distance between medial edges of joint surfaces of both OCs

- **Maximum bicondylar distance (MaxBD):** Maximum distance between lateral joint surface edges of both OCs
- **Sagittal intercondylar angle (total SICA):** Angle between the long axes of the right and left OCs
- **Right and left sagittal condylar angle (right SCA – left SCA):** Angle between condylar long axis and sagittal midline
- **Distance between anterior tip of right OC and B (right OCAT-B)**
- **Distance between anterior tip of left OC and B (left OCAT-B)**
- **Distance between posterior tip of right OC and B (right OCPT-B)**
- **Distance between posterior tip of left OC and B (left OCPT-B),**
- **Distance between anterior tip of right OC and O (right OCAT-O)**
- **Distance between anterior tip of left OC and O (left OCAT-O),**
- **Distance between posterior tip of right OC and O (right OCPT-O)**
- **Distance between posterior tip of left OC and O (left OCPT-O).**

### **Statistical analysis**

Data were evaluated using SPSS 25.0 [IBM SPSS Statistics 25 software (Armonk, NY: IBM Corporation)]. Continuous variables are presented as mean  $\pm$  standard deviation, median (25<sup>th</sup>-75<sup>th</sup> percentile: IQR), min-max, and categorical variables are presented as numbers and percentages. To test the suitability of the data for normal distribution, the Kolmogorov-Smirnov test was used. In examining the differences between groups, independent samples t test was used when parametric test assumptions were met, and the Mann Whitney U test was used when parametric test assumptions were not met. Differences between categorical variables were examined with Chi square analysis. In dependent group comparisons, paired samples t test was used when parametric test assumptions were met. Intraclass correlation coefficient (ICC-ICC) was used to examine the reliability of the measurements taken. Discriminant Analysis method was used to determine sex differences. In discriminant analysis models, canonical correlation coefficients (CCC), Wilks lambda' values and explained variance values were examined. As a result of the univariate examinations, different multivariate models were used, both clinically and statistically, and model equations were created using the results of the models with the highest discrimination values. The same observer re-evaluated 10 randomly selected carotid angio-CT images to evaluate the intra-observer agreement. Intra-observer agreement was analysed using intraclass correlation coefficient (ICC)

scores with a 95% confidence interval (ICC score range: 0.91-1). In all analyses,  $p < 0.05$  was considered statistically significant.

## Results

The study included 481 cases, 189 females (39.3%) and 292 males (60.7%). Mean age was  $56.64 \pm 14.22$  (min-max: 19-87) in females and  $58.84 \pm 14.26$  (min-max: 19-89) in males. With the exception of the left SCA, all measurements of the right and left OCs were significantly different between the male and female cases ( $p < 0.05$ ). Right OCL, left OCL, right OCW, left OCW, right OCH, left OCH, AID, PID, MaxID, MinID, MaxBD, right OCAT-B, left OCAT-B, right OCPT-B, left OCPT-B, right OCAT-O, left OCAT-O, right OCPT-O, left OCPT-O measurements were greater in the male cases than in the female cases. Right BCI, left BCI, right SCA, total SICA measurements were greater in the female cases than in the male cases ( $p < 0.05$ ) (Table 1).

The results of the univariate discriminant function analysis used to analyse sex differences are shown in Table 2. The accuracy of sex classification of the variables with the highest variance explaining value were 85.3% in males and 53.4% in females in left OCAT-O; 82.5% in males and 55.6% in females in right OCL; 80.8% in males and 56.1% in females in left OCL; 79.8% in males and 52.4% in females in maxBD (Table 2).

With the exception of the right SCA, the left SCA, total SICA, the right BCI and the left BCI, the multivariate discriminant function analysis was performed by creating different models with variables (Table 3). The multivariate analysis showed an accuracy percentage ranging from 81.2% to 84.6% in males and from 52.9% to 68.8% in females. Function 15 had the highest accuracy in classifying sex (males: 84.6%; females: 68.8%), followed by function 14, 13, 12 and 11, respectively. The constants and variable coefficients of these functions are shown in Table 4.

When comparing the results obtained by calculating the values of the relevant variables by substituting them into the two equations given separately for male and female, the larger result indicates the estimated sex. The discriminant function equation for function 15 with the highest value of explanatory variance:

$$\text{Male} = -276.174 - 1.063(\text{AID}) - 2.231(\text{PID}) + 3.257(\text{MaxID}) + 1.941(\text{MinID}) - 0.378(\text{MaxBD}) + 1.385(\text{left OCL}) + 5.012(\text{left OCW}) - 0.659(\text{left OCH}) + 0.684(\text{left OCAT-B}) + 1.069(\text{left OCPT-B}) + 0.316(\text{left OCAT-O}) + 1.931(\text{left OCPT-O}) +$$

0.114(right OCL) + 3.307(right OCW) + 5.165(right OCH) + 0.002(right OCAT-B) + 3.910(right OCPT-B) + 1.886(right OCAT-O) + 0.732(right OCPT-O)

Female= -243.940 – 1.190(AID) - 2.181(PID) + 3.100(MaxID) + 1.912(MinID) – 0.433(MaxBD) + 0.948(left OCL) + 4.646(left OCW) – 0.574(left OCH) + 0.474(left OCAT-B) + 1.312(left OCPT-B) + 0.312(left OCAT-O) + 1.630(left OCPT-O) – 0.078(right OCL) + 3.201(right OCW) + 5.066(right OCH) – 0.068(right OCAT-B) + 3.781(right OCPT-B) + 1.843(right OCAT-O) + 0.821 (right OCPT-O)

## Discussion

There are many studies that have performed morphometrical analysis of the occipital condyles for anatomical, clinical and forensic purposes [8, 12, 13-24]. In the literature, morphometric evaluation of the occipital condyle has been performed on the skull [12, 13, 15-20], on CT images of the skull [21, 24] and only in a few studies on 3D CT models [8, 14]. In the study by Avci et al. [25], measurements were taken from both bone tissue and 3D CT images of the dry skull and the results were compared. In this study, occipital condyles were analysed for sex differences in 3D models of carotid angio-CT images of living subjects.

In this study, sexual dymorphism was followed in the parameters of the OC, except for the left SCA. The measurement values of all parameters with sexual dimorphism (except right SCA, total SICA, right and left BCI) were higher in males than in females ( $p < 0.05$ ). These results were found to be similar to most studies in the literature [8, 12, 13-18, 20-22, 24]. However, in the study by Natsis et al. [19], there was no statistically significant difference between sex and right and left occipital condyle width. There was no statistically significant difference between left OCW and sex in study by Abo El-Atta et al. [23]. Çiçekçibaşı et al. [13] found no statistically significant different in mean total SICA between sexes.

Comparison of occipital condyle measurements in different populations is shown in Table 5. When the mean values of the occipital condyle measurements are examined, it can be seen that they are similar to many population studies [8, 12, 13, 15, 17, 18-21]. However, our results also differed from those of some populations [14, 16, 22-24]. It has been suggested that the differences between the mean values of the same variables in different studies may be due to reasons such as methodological differences and population differences.

In our study, the right OCPT-B was the best measure for sex estimation in univariate discriminant function analyses with an accuracy rate of 73.3%. In the

multivariate discriminant function analyses, the correct classification percentages of the models with the highest variance explanation value were between 77.1% and 78.4%, ranging from 81.2% to 84.6% for males and 52.9% to 68.8% for females. Aljarrah et al. [24] reported that multivariate analysis including all eight variables of FM and OC predicted sex with an accuracy of 71.6% (73.3% for males and 69.9% for females). In a study by Gapert et al. (2009) [12], the most successful single variable for predicting sex was the maximum bicondylar distance with 69.2%. In a multivariate discriminant function analysis, the highest accuracy rate (76.7%, male: 72%, female: 81.7%) was obtained in the model including the variables left OC length, right OC width and minimum intercondylar distance [12]. In the study by Macaluso et al. [15], the most effective single variable for sex prediction was the maximum bicondylar distance with 67.6% (male: 61.1%, female: 75%). A stepwise analysis using the maximum length of the left OC and the minimum distance between OCs showed the highest classification accuracy of 67.7% (male: 68.6% - female: 66.7%) [15]. In El-Barrany et al. [21], discriminant function analyses showed that the minimum intercondylar distance, right OC length and foramen magnum width were the main variables in sex prediction. In the function including these variables, the correct prediction rate was found to be 84.3% in all cases, 81% in males and 87.5% in females [21]. Abo El-Atta et al. [23] reported that most significant discriminating variables in prediction of sex were right OC length and foramen magnum width. They found that the sex prediction accuracy rate was 66.5% (male: 63.2%- female: 69.1%) for right OC length. In a multivariate discriminant function analysis, they achieved a correct classification rate of 70.9% (male: 59.3%- female: 80.2%) [23]. In Madadin et al. [22], correct sex classification in univariate and multivariate discriminant function analysis ranged from 51%-71%. The highest correct sex classification rate (male 70%, female 72%, total 71%) was obtained in the model that included the variables of right and left OC length and width and maximum bicondylar distance [22]. In the study by Singh and Talwar [26], the accuracy of predicting sex on the bases of discriminant function analysis was reported to be between 66% and 70%. Uysal et al. [27] reporting an accurate rate of 81% for sex determination using the model including right OCL and OCW and FM width.

In conclusion, in present study, morphometric analysis of OCs in the contemporary Turkish population revealed sexual dimorphism in all parameters except the left sagittal condylar angle. In the multivariate functional analysis, the correct sex prediction rate of the occipital condyles was 77.1% to 78.4% (81.2% to



84.6% in males and 52.9% to 68.8% in females). This study showed that measurements from 3D CT images of occipital condyles can be used for sex estimation. Thus, 3D modelling of cranial CT images will help to create databases to study population-specific differences in contemporary societies and to use these data for sex determination in forensic investigations, as it provides the opportunity to examine the skulls of living individuals with known sex, age and medical history.

This study was prepared by reorganising the doctoral thesis entitled "Evaluation of sex with occipital condyle measurements on three-dimensional computed tomography images" by the author named Harun Yıldız.

**Funding:** None

**Authors contributions:** A.K.D. and H.Y. constructed the main idea and hypothesis of the study. H.Y. and E.S. developed the theory and arranged/edited the material and method section. H.Y. and H.Ş. and have done the evaluation of the data in the Results section. Discussion section of the article written by H.Y. A.K.D. reviewed, corrected and approved. In addition, all authors discussed the entire study and approved the final version.

**Conflict of interest:** No conflict of interest was declared by the authors.

## References

1. Saukko P, Knight B. Knight's forensic pathology. London: *CRC Press*. 2016:103-107.
2. Kemkes Grotenthaler A. The reliability of forensic osteology--a case in point. Case study. *Forensic Sci Int*. 2001;117(1-2):65-72. doi:10.1016/s0379-0738(00)00450-3
3. Spradley MK, Jantz RL. Sex estimation in forensic anthropology: skull versus postcranial elements. *J Forensic Sci*. 2011;56(2):289-296. doi:10.1111/j.1556-4029.2010.01635.x
4. Gonzalez P, Bernal V, Perez S. Analysis of sexual dimorphism of craniofacial traits using geometric morphometric techniques. *Int J Osteoarchaeol*. 2011;21:82-91. doi:10.1002/oa.1109
5. Saini V, Srivastava R, Rai RK, Shamal SN, Singh TB, Tripathi SK. Mandibular ramus: an indicator for sex in fragmentary mandible. *J Forensic Sci*. 2011;56 Suppl 1:S13-S16. doi:10.1111/j.1556-4029.2010.01599.x
6. Bruzek J, Murail P. Methodology and reliability of sex determination from the skeleton. In: Schmitt A, Cunha E, Pinheiro J, eds. *Forensic anthropology and medicine*. New Jersey: *Humana Press*. 2006:225-242. doi:10.1007/978-1-59745-099-7\_9

7. Sholapurkar VT, Virupaxi RD, Desai SP. Morphometric analysis of human occipital condyles for sex determination in dry adult skulls. *Int J Anat Res.* 2017;5:3318-3341. doi:10.16965/ijar.2016.457
8. Abdel Karim RI, Housseini AM, Hashish RK. Adult sex estimation using three dimensional volume rendering multislice computed tomography of the foramen magnum and occipital condyles: A study in Egyptian population. *Int. J. of Adv. Res.* 2015;3:1212-1215.
9. Gapert R, Black S, Last J. Sex determination from the foramen magnum: discriminant function analysis in an eighteenth and nineteenth century British sample. *Int J Legal Med.* 2009;123(1):25-33. doi:10.1007/s00414-008-0256-0
10. Dirnhofer R, Jackowski C, Vock P, Potter K, Thali MJ. VIRTOPSY: minimally invasive, imaging-guided virtual autopsy. *Radiographics.* 2006;26(5):1305-1333. doi:10.1148/rg.265065001
11. Dereli AK, Zeybek V, Sagtas E, Senol H, Ozgul HA, Acar K. Sex determination with morphological characteristics of the skull by using 3D modeling techniques in computerized tomography. *Forensic Sci Med Pathol.* 2018;14(4):450-459. doi:10.1007/s12024-018-0029-0
12. Gapert R, Black S, Last J. Sex determination from the occipital condyle: discriminant function analysis in an eighteenth and nineteenth century British sample. *Am J Phys Anthropol.* 2009;138(4):384-394. doi:10.1002/ajpa.20946
13. Çiçekcibaşı AE, Murshid KA, Ziylan T, Şeker M, Tuncer I. A morphometric evaluation of some important bony landmarks on the skull base related to sexes. *Turk J Med Sci.* 2004;34:37-42.
14. Gumussoy I, Duman SB. Morphometric analysis of occipital condyles using alternative imaging technique. *Surg Radiol Anat.* 2020;42:161-169. doi:10.1007/s00276-019-02344-2
15. Macaluso PJ. Metric sex determination from the basal region of the occipital bone in a documented french sample. *Bull. Mém. Soc. Anthropol.* 2010;23:19-26. doi:10.1007/s13219-010-0023-x
16. Kalthur SG, Padmashali S, Gupta C, Dsouza AS. Anatomic study of the occipital condyle and its surgical implications in transcondylar approach. *J Craniovertebr Junction Spine.* 2014;5(2):71-77. doi:10.4103/0974-8237.139201
17. Kumar A, Nagar M. Human adult occipital condyles: a morphometric analysis. *Res Rev J Med Health Sci.* 2014;3:112-116.

18. Oliveira OF, Tinoco RLR, Daruge Júnior E, Araujo LG, Silva RHA, Paranhos LR. Sex determination from occipital condylar measurements by baudoin index in forensic purposes. *Int. J. Morphol.* 2013;31:1297-1300. doi:10.4067/S0717-95022013000400024
19. Natsis K, Piagkou M, Skotsimara G, Piagkos G, Skandalakis P. A morphometric anatomical and comparative study of the foramen magnum region in a Greek population. *Surg Radiol Anat.* 2013;35(10):925-934. doi:10.1007/s00276-013-1119-z
20. Lyrtzis C, Piagkou M, Gkioka A, Anastasopoulos N, Apostolidis S, Natsis K. Foramen magnum, occipital condyles and hypoglossal canals morphometry: anatomical study with clinical implications. *Folia Morphol (Warsz).* 2017;76(3):446-457. doi:10.5603/FM.a2017.0002
21. El Barrany UM, Ghaleb SS, Ibrahim SF, Nouri M, Mohammed AH. Sex prediction using foramen magnum and occipital condyles computed tomography measurements in Sudanese population. *AJFSFM.* 2016;230.3950:1-9. doi:10.12816/0033135
22. Madadin M, Menezes RG, Al Saif HS, et al. Morphometric evaluation of the foramen magnum for sex determination: A study from Saudi Arabia. *J Forensic Leg Med.* 2017;46:66-71. doi:10.1016/j.jflm.2017.01.001
23. Abo El Atta HMH, Abdel Rahman RH, El Hawary G, Abo El Al Atta HM. Sexual dimorphism of foramen magnum: an Egyptian study. *Egypt J Forensic Sci.* 2020;10:1-12. doi:10.1186/s41935-019-0167-x
24. Aljarrah K, Packirisamy V, Al Anazi N, Nayak SB. Morphometric analysis of foramen magnum and occipital condyle using CT images for sex determination in a Saudi Arabian population. *Morphologie.* 2022;106(355):260-270. doi:10.1016/j.morpho.2021.07.006
25. Avci E, Dagtekin A, Ozturk AH, et al. Anatomical variations of the foramen magnum, occipital condyle and jugular tubercle. *Turk Neurosurg.* 2011;21(2):181-190. doi:10.5137/1019-5149.JTN.3838-10.1
26. Singh G, Talwar I. Morphometric analysis of foramen magnum in human skull for sex determination. *Hum Bio Rev.* 2013;2:29-41.
27. Uysal S, Gokharman D, Kacar M, Tuncbilek I, Kosa U. Estimation of sex by 3D CT measurements of the foramen magnum. *J Forensic Sci.* 2005;50(6):1310-1314.

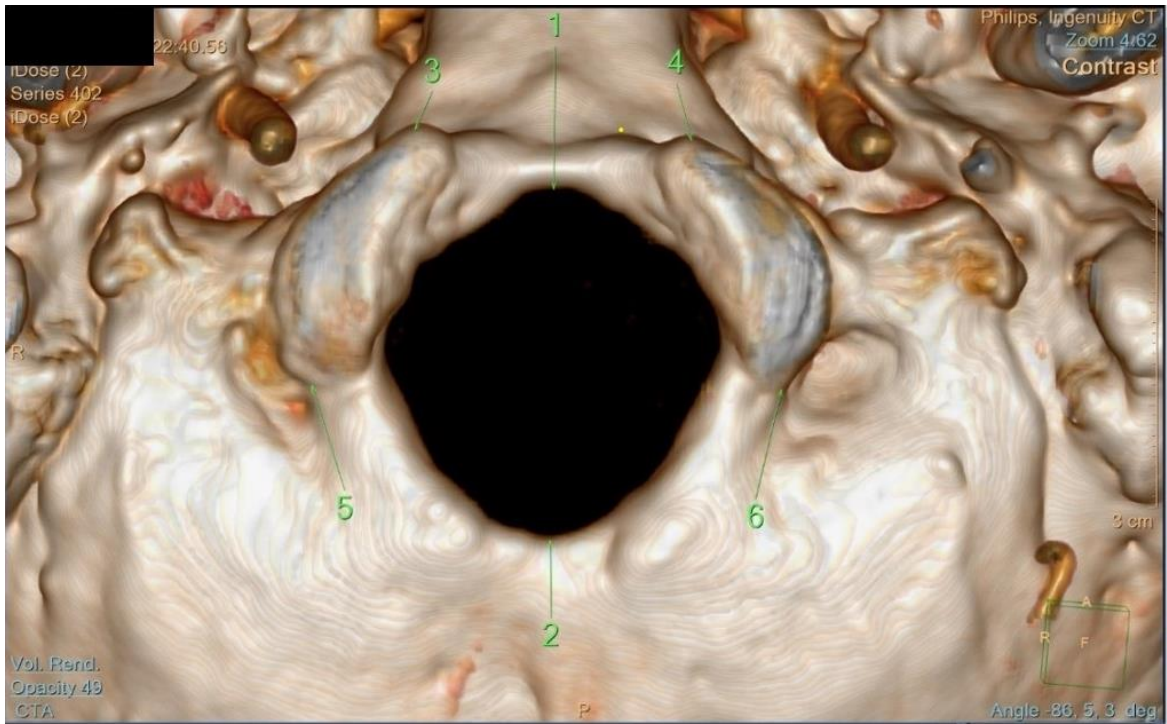


**Figure 1.** Landmarks used in present study

1. Basion (B), 2. Opisthion (O), 3. The anterior tip of the right occipital condyle (right OCAT)
4. The anterior tip of the left occipital condyle (left OCAT), 5. The posterior tip of the right occipital condyle (right OCPT), 6. The posterior tip of the left occipital condyle (left OCPT)

**Table 1. Descriptive statistical analysis results**

	Males			Females			p
	Mean±SD	Med (IQR)	Min-max	Mean±SD	Med (IQR)	Min-max	
right OCL	25.55±2.24	25.8 (24.13-27.1)	17.7-31.5	23.29±1.97	23.3 (22-24.65)	18.2-30.7	0.0001* (t=11.294)
left OCL	25.51±2.46	25.6 (23.83-27.18)	17.8-31.1	23.22±1.93	23.1 (21.85-24.6)	18.1-28.3	0.0001* (t=11.408)
right OCW	11.69±1.38	11.6 (10.7-12.6)	8.6-15.9	11.11±1.25	11 (10.3-11.75)	8.3-15	0.0001* (z=-4.753)
left OCW	11.9±1.33	11.8 (11-12.8)	8.9-16.2	11.19±1.41	11 (10.2-11.95)	8.4-16	0.0001* (z=-5.893)
right BCI	46.14±7.04	45.13 (41.21-50.15)	30.94-77.18	48.09±7.19	47.3 (43.06-52.28)	35.43-72.5	0.003* (z=-3.022)
left BCI	47.14±7.6	46.23 (41.9-51.21)	31.94-78.09	48.58±7.64	47.11 (43.69-52.95)	35.11-77.78	0.033* (z=-2.13)
right OCH	10.08±1.46	9.9 (9.03-11.08)	6.9-14.9	9.66±1.22	9.6 (8.8-10.5)	6-13.2	0.003* (z=-2.954)
left OCH	10.08±1.46	9.9 (9-11)	6.9-14.6	9.5±1.24	9.6 (8.6-10.4)	6-12.1	0.0001* (z=-3.496)
AID	22.77±2.75	22.7 (21.2-24.4)	15.1-33.5	21.09±2.45	21 (19.4-22.6)	12.1-29.3	0.0001* (t=6.821)
PID	45.08±3.46	45.2 (42.6-47.5)	35.9-54.2	42.29±3.59	42.1 (39.9-44.5)	34.8-52.2	0.0001* (z=-8.041)
MaxID	33.92±2.37	33.9 (32.23-35.4)	25.6-40.1	32.01±2.31	32 (30.4-33.6)	26.9-39.3	0.0001* (t=8.731)
MinID	21.35±2.48	21.3 (19.8-22.8)	13.6-28.6	19.91±2.19	19.9 (18.4-21.45)	14.1-27.3	0.0001* (t=6.529)
MaxBD	51.25±3.13	50.9 (48.93-53.28)	42.3-59.5	48.13±3.18	48.2 (45.7-50.15)	39.9-55.8	0.0001* (t=10.607)
right SCA	26.56±5.74	26 (23-30)	10-48	28.13±6.1	27 (24-32)	11-49	0.004* (z=-2.915)
left SCA	27.5±6.34	27 (23-31)	5-47	28.17±5.81	28 (24-31)	15-48	0.169 (z=-1.376)
total SICA	54.06±10.6	53 (47-60)	22-89	56.3±10.69	55 (49-62)	34-94	0.016* (z=-2.405)
right OCAT-B	13.28±1.65	13.15 (12.1-14.2)	9-22	12.19±1.29	12.2 (11.3-13)	8.5-16.2	0.0001* (t=8.104)
left OCAT-B	13.35±1.71	13.2 (12.23-14.4)	9-22.4	12.26±1.35	12.2 (11.25-13.2)	9.4-17.7	0.0001* (z=-7.237)
right OCPT-B	29.44±1.93	29.3 (28.3-30.68)	28.3-30.6	27.49±1.91	27.4 (26.2-29)	20.1-33.3	0.0001* (z=-9.73)
left OCPT-B	29.42±1.98	29.5 (28.03-30.6)	23.8-34.6	27.5±2.08	27.4 (26.1-28.8)	22.5-39.8	0.0001* (t=10.152)
right OCAT-O	41.12±3.14	41.3 (39.4-43.1)	26.1-51.2	38.3±2.7	38.4 (36.55-40.3)	25.9-43.5	0.0001* (t=10.16)
left OCAT-O	41.4±2.96	41.5 (39.7-43.1)	26.8-51.6	38.45±2.43	38.5 (36.5-40.3)	32.4-44.1	0.0001* (t=11.446)
right OCPT-O	28.41±2.76	28.25 (26.7-29.6)	21.7-42.2	27.03±2.58	26.8 (25.15-29.1)	19.6-34	0.0001* (z=-4.984)
left OCPT-O	28.89±2.71	28.8 (27.2-30.58)	21.1-42.2	27.09±2.47	26.9 (25.4-28.85)	21.3-36.1	0.0001* (t=7.381)

\* $p < 0.05$  statistical significance difference; SD: Standard deviation; Med (IQR): Median (25<sup>th</sup>-75<sup>th</sup> percentile); Min: Minimum; max: Maximum; t: Independent Sample T test; z: Mann Whitney U test

**Table 2.** Univariate discriminant function analysis results

Variables	Sexing Accuracy Rates			CCC	Wilks' Lambda	<i>p</i>	Explained Variance (%)
	Male (n=292)	Female (n=189)	Total				
right OCL	241 (82.5%)	105 (55.6%)	346 (71.9%)	0.459	0.79	0.0001*	21.1
left OCL	236 (80.8%)	106 (56.1%)	342 (71.1%)	0.444	0.803	0.0001*	19.7
right OCW	259 (88.7%)	36 (19%)	295 (61.3%)	0.208	0.957	0.0001*	4.3
left OCW	250 (85.6%)	59 (31.2%)	309 (64.2%)	0.246	0.94	0.0001*	6.1
right BCI	275 (94.2%)	17 (9%)	292 (60.7%)	0.134	0.982	0.003*	1.8
left BCI	285 (97.6%)	7 (3.7%)	292 (60.7%)	0.092	0.992	0.043*	0.8
right OCH	274 (93.8%)	11 (5.8%)	285 (59.2%)	0.146	0.979	0.001*	2.1
left OCH	267 (91.4%)	31 (16.4%)	298 (61.9%)	0.201	0.96	0.0001*	4
AID	246 (84.2%)	63 (33.3%)	309 (64.2%)	0.298	0.911	0.0001*	8.9
PID	241 (82.5%)	89 (47.1%)	330 (68.6%)	0.363	0.869	0.0001*	13.2
MaxID	246 (84.2%)	91 (48.1%)	337 (70.0%)	0.371	0.863	0.0001*	13.8
MinID	244 (83.6%)	61 (32.3%)	305 (63.4%)	0.286	0.918	0.0001*	8.2
MaxBD	233 (79.8%)	99 (52.4%)	332 (69.0%)	0.436	0.81	0.0001*	19
right SCA	278 (95.2%)	17 (9%)	295 (61.3%)	0.13	0.983	0.004*	1.7
left SCA	292 (100%)	189 (0%)	292 (0.6%)	0.054	0.997	0.241	0.3
total SICA	283 (96.9%)	9 (4.8%)	292 (60.7%)	0.103	0.989	0.024*	1.1
right OCAT-B	242 (82.9%)	73 (38.6%)	315 (65.4%)	0.332	0.89	0.0001*	11
left OCAT-B	247 (84.6%)	74 (39.2%)	321 (66.7%)	0.319	0.898	0.0001*	10.2
right OCPT-B	247 (84.6%)	106 (56.1%)	353 (73.3%)	0.444	0.803	0.0001*	19.7
left OCPT-B	242 (82.9%)	98 (51.9%)	340 (70.6%)	0.421	0.823	0.0001*	17.7
right OCAT-O	252 (86.3%)	93 (49.2%)	345 (71.7%)	0.421	0.823	0.0001*	17.7
left OCAT-O	249 (85.3%)	101 (53.4%)	350 (72.7%)	0.463	0.785	0.0001*	21.4
right OCPT-O	261 (89.4%)	52 (27.5%)	313 (65.0%)	0.244	0.94	0.0001*	6
left OCPT-O	246 (84.2%)	77 (40.7%)	323 (67.1%)	0.32	0.898	0.0001*	10.2

\**p*<0.05 statistical significance difference; CCC: Canonical Correlation Coefficient, Wilk's Lambda coefficient

**Table 3. Multivariate discriminant function analysis**

Functions	Variables	Sexing Accuracy Rates		CCC	Wilks' Lambda	<i>p</i>	Explained Variance (%)
		Male (n=292) n (%)	Female (n=189) n (%)				
Function 1	right OCL, left OCL, right OCW, left OCW	240 (82.2%)	113 (59.8%)	0.52	0.729	0.0001*	27.1
Function 2	right OCL, left OCL, right OCW, left OCW, right OCH, left OCH	242 (82.9%)	112 (59.3%)	0.523	0.726	0.0001*	27.4
Function 3	AID, PID, MaxID, MinID, MaxBD	244 (83.6%)	100 (52.9%)	0.474	0.775	0.0001*	22.5
Function 4	right OCAT-B, left OCAT-B, right OCPT-B, left OCPT-B	237 (81.2%)	115 (60.8%)	0.5	0.75	0.0001*	25
Function 5	right OCAT-O, left OCAT-O, right OCPT-O, left OCPT-O	246 (84.2%)	102 (54%)	0.481	0.769	0.0001*	23.1
Function 6	right OCAT-B, left OCAT-B, right OCPT-B, left OCPT-B, right OCAT-O, left OCAT-O, right OCPT-O, left OCPT-O	241 (82.5%)	123 (65.1%)	0.562	0.684	0.0001*	31.6
Function 7	right OCL, right OCW, right OCH	240 (82.2%)	118 (62.4%)	0.493	0.757	0.0001*	24.3
Function 8	left OCL, left OCW, left OCH	239 (81.8%)	114 (60.3%)	0.501	0.749	0.0001*	25.1
Function 9	right OCAT-B, right OCPT-B, right OCAT-O, right OCPT-O	243 (83.2%)	108 (57.1%)	0.537	0.711	0.0001*	28.9
Function 10	left OCAT-B, left OCPT-B, left OCAT-O, left OCPT-O	238 (81.5%)	119 (63%)	0.541	0.708	0.0001*	29.2
Function 11	right OCL, right OCW, right OCH, right OCAT-B, right OCPT-B, right OCAT-O, right OCPT-O	244 (83.6%)	127 (67.2%)	0.576	0.668	0.0001*	33.2
Function 12	left OCL, left OCW, left OCH, left OCAT-B, left OCPT-B, left OCAT-O, left OCPT-O	245 (83.9%)	130 (68.8%)	0.598	0.643	0.0001*	35.7
Function 13	right OCL, right OCW, right OCH, AID, PID, MaxID, MinID, MaxBD, right OCAT-B, right OCPT-B, right OCAT-O, right OCPT-O	246 (84.2%)	127 (67.2%)	0.587	0.655	0.0001*	34.5
Function 14	left OCL, left OCW, left OCH, AID, PID, MaxID, MinID, MaxBD, left OCAT-B, left OCPT-B, left OCAT-O, left OCPT-O	243 (83.2%)	130 (68.8%)	0.61	0.628	0.0001*	37.2
Function 15	AID, PID, MaxID, MinID, MaxBD, left OCL, left OCW, left OCH, left OCAT-B, left OCPT-B, left OCAT-O, left OCPT-O, right OCL, right OCW, right OCH, right OCAT-B, right OCPT-B, right OCAT-O, right OCPT-O	247 (84.6%)	130 (68.8%)	0.622	0.613	0.0001*	38.7

\**p*<0.05 statistical significance difference; CCC: Canonical Correlation Coefficient, Wilk's Lambda coefficient

**Table 4.** The discriminant equations coefficients for functions 11-15

	Function 11		Function 12		Function 13		Function 14		Function 15	
	Male	Female	Male	Female	Male	Female	Male	Female	Male	Female
AID					-.752	-.845	-.061	-.233	-1.063	-1.190
PID					-.825	-.872	-.505	-.475	-2.231	-2.181
MaxID					2.842	2.728	3.121	2.980	3.257	3.100
MinID					1.749	1.719	1.132	1.140	1.941	1.912
MaxBD					.945	.934	.633	.659	.378	.433
left OCL			.659	.206			1.171	.618	1.385	.948
left OCW			5.961	5.590			6.790	6.367	5.012	4.646
left OCH			3.116	3.072			2.888	2.866	-.659	-.574
left OCAT-B			1.755	1.337			.089	-.144	.684	.474
left OCPT-B			3.807	3.902			2.294	2.476	1.069	1.312
left OCAT-O			3.759	3.627			3.086	3.008	.316	.312
left OCPT-O			1.220	1.035			.775	.566	1.931	1.630
right OCL	.585	.218			.995	.564			.114	-.078
right OCW	5.502	5.235			6.144	5.856			3.307	3.201
right OCH	4.662	4.580			4.781	4.703			5.165	5.066
right OCAT-B	2.078	1.695			.459	.233			.002	-.068
right OCPT-B	4.809	4.718			3.319	3.384			3.910	3.781
right OCAT-O	2.973	2.847			2.389	2.292			1.886	1.843
right OCPT-O	1.461	1.384			1.243	1.208			.732	.821
Constant	-230.074	-203.096	-223.198	-194.799	-255.805	-226.806	-248.955	-218.424	-276.174	-243.940



**Table 5.** Comparison of the measurements of the occipital condyles in the present study with the results of other studies

Studies	Population	Material	right OCL		left OCL		right OCW		left OCW		right OCH		left OCH		AID		PID		MaxID		MinID		MaxBD		
			M	F	M	F	M	F	M	F	M	F	M	F	M	F	M	F	M	F	M	F	M	F	
Present study	Turkish	3DCT	25.55±2.24	23.29±1.97	25.51±2.46	23.22±1.93	11.69±1.38	11.11±1.25	11.9±1.33	11.19±1.41	10.0±1.46	9.66±1.22	10.08±1.46	9.50±1.24	22.77±2.75	21.09±2.45	45.08±3.46	42.29±3.59	33.92±2.37	32.01±2.31	21.35±2.48	19.91±2.19	51.25±3.13	48.13±3.18	
Çiçekçibaşı et al. [13]	Turkish	Dry skull	25.13±2.36	23.44±1.90	24.82±2.43	23.17±1.89									16.09±1.93	14.68±1.80									
Gapert et al. [12]	British	Dry skull	24.95±2.53	23.30±2.28	25.16±2.51	23.74±2.44	12.01±1.41	11.42±1.21	12.05±1.69	11.57±1.16									36.82±3.10	35.12±3.09	21.12±3.18	19.0±2.40	51.29±2.97	48.67±3.17	
Macaluso et al. [15]	France	Dry skull	24.62±2.65	22.99±2.28	24.99±3.09	22.88±2.69	12.30±1.27	11.59±1.03	12.25±1.51	11.57±1.09									37.46±3.54	36.78±3.69	20.63±3.18	19.07±2.14	51.32±3.70	48.73±3.27	
Oliviera et al. [18]	Brazil	Dry skull	26.74±2.96	25.45±3.21	26.85±2.97	24.65±3.23	13.51±1.38	12.68±1.56	13.79±1.39	12.71±1.75															
Natsis et al. [19]	Greek	Dry skull	26.30±2.92	24.70±2.66	26.48±2.80	24.57±2.13	13.13±2.01	13.04±1.99	13.24±2.20	12.74±1.63					19.82±3.19	18.77±3.26	52.8±4.93	50.13±4.71							
Lyrztis et al. [20]	Greek	Dry skull	24.33±2.57	22.95±2.96	24.07±2.59	23.23±2.71	12.10±1.50	11.43±1.47	12.21±1.66	11.46±1.51					21.17±2.71	20.05±2.45	43.36±3.35	41.23±3.30							
Kumar et al. [17]	Indian	Dry skull	23.88±1.50	22.60±1.30	24.99±1.82	24.20±1.62	12.97±1.43	12.65±1.33	14.11±1.01	13.85±1.02	8.64±0.74	6.92±0.72	9.32±0.78	9.21±0.76	17.63	17.30									
Kalthur et al. [16]	Indian	Dry skull	22.8±2.5	21.4±2.9	22.9±2.4	21.6±2.6	10.5±1.8	12.0±2.3	10.8±2.4	12.2±2.6					21±03	22±03	38±3	39±3	26±3	25±2			45±4	46±3	
Singh and Talwar [26]	Indian	Dry skull																	26.15±3.31	24.71±4.57	14.88±2.26	14.33±2.56	46.73±2.79	44.29±2.34	
El- barrany et al. [21]	Sudanese	CT	25.52±2.68	21.41±2.05	25.40±3.04	21.50±2.19	11.39±1.51	10.62±1.34	11.33±1.71	10.38±1.33									27.20±2.74	25.46±2.50	10.49±2.63	9.62±2.15	48.90±4.73	46.89±4.02	
Madadin et al. [22]	Saudi Arabian	CT	21.10±1.55	19.94±1.81	21.11±1.72	20.05±1.82	10.58±1.08	10.27±1.30	10.72±1.16	10.48±1.31														43.67±2.93	43.45±3.77
Abo El-Atta et al. [23]	Egyptian	CT	20.8±2.4	18.9±2.5	20.7±2.4	19.7±2.2	11.6±1.3	11.1±1.4	11.2±1.3	11.3±1.2									28.9±5.9	27.2±4.9	15.4±9.0	13.7±3.1			
Aljarrah et al. [24]	Saudi Arabian	CT	22.02±2.2	20.9±2	21.3±2	20.2±1.9	11.3±1.40	10.99±1.41	11.43±1.36	11.2±1.37															
Gümüşsoy et al. [14]	Turkish	CT -3DCT	21.0±1.8	18.8±1.7	20.5±2.0	18.9±1.6	10.7±1.2	9.9±1.1	10.9±1.4	10.2±1.2	9.5±2.0	8.9±1.2	9.4±1.4	8.7±1.0	21.6± 1.1	20.3±1.8	44.6±1.7	43.4±2.2							
Abdel-karim et al. [8]	Egyptian	3DCT	26.91±2.41	24±1.33	27.09±2.55	23.67±1.43	12.22±1.33	11.13±1.11	11.91±1.20	10.75±1.18									31.57±3.27	30.42±2.10	7.22±1.33	6.83±0.86	51.09±3.35	49.54±3.03	

OCL: Occipital condyle length, OCW: Occipital condyle width, OCH: Occipital condyle height, AID: Anterior intercondylar distance, PID: Posterior intercondylar distance, MaxID: Maximum intercondylar distance, MinID: Minimum intercondylar distance, MaxBD: Maximum bicondylar distance, M: male, F: female

Yildiz H, Kurtulus Dereli A, Sagtas E, Senol H. Determination of sex with occipital condyle measurements on three-dimensional computed tomography images. Pam Med J 2025;18:....-...

Yıldız H, Kurtuluş Dereli A, Sağtaş E, Şenol H. Üç boyutlu bilgisayarlı tomografi görüntülerinde oksipital kondil ölçümleri ile cinsiyetin değerlendirilmesi. Pam Tıp Derg 2025;18:....-...

Harun Yıldız, M.D. Mardin Forensic Medicine Branch Directorate, Mardin, Türkiye, e-mail: drhnyldz@hotmail.com (<https://orcid.org/0000-0001-6614-0389>) (Corresponding Author)

Ayşe Kurtulus Dereli, Prof. Pamukkale University, Faculty of Medicine, Department of Forensic Medicine, Denizli, Türkiye, e-mail: akurtulus@pau.edu.tr (<https://orcid.org/0000-0002-0592-585X>)

Ergin Sağtaş, Assoc. Prof. Pamukkale University, Faculty of Medicine, Department of Radiology, Denizli, Türkiye, e-mail: esagtas@pau.edu.tr (<https://orcid.org/0000-0001-6723-6593>)

Hande Şenol, Asst. Prof. Pamukkale University, Faculty of Medicine, Department of Biostatistics, Denizli, Türkiye, e-mail: hsenol@pau.edu.tr (<https://orcid.org/0000-0001-6395-7924>)